Supplements

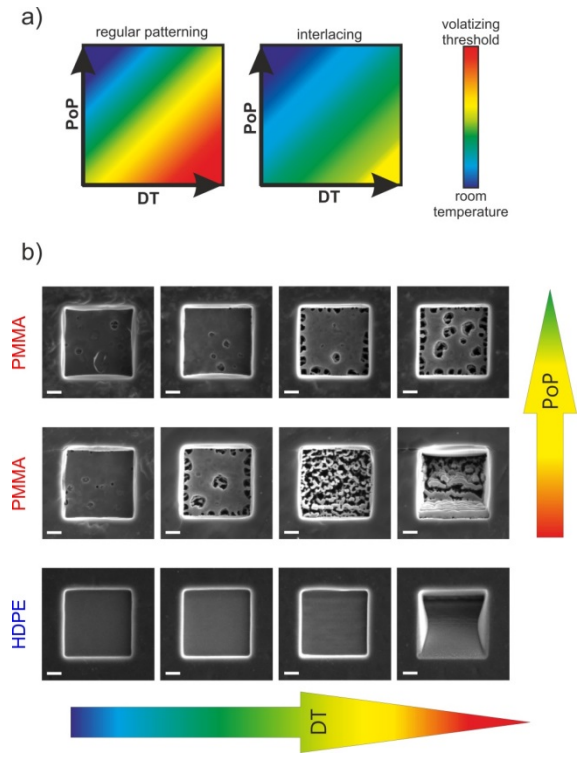

Figure S 1: a) qualitative scheme of the different temperatures reached due to heat accumulation in dependence on the dwell time (DT) and the point pitch (PoP) for regular patterning (left) and interlacing (right) derived from resulting morphology regimes (see b) and from results shown in [**Error! Bookmark not defined.**]. b) SEM images of the morphologies for regularly patterned PMMA (top and middle row) and HDPE (bottom row), with increasing DTs from left to right and for PMMA also for two different point pitches – 40 nm (top) and 20 nm (middle). Scale bars are 1 µm.

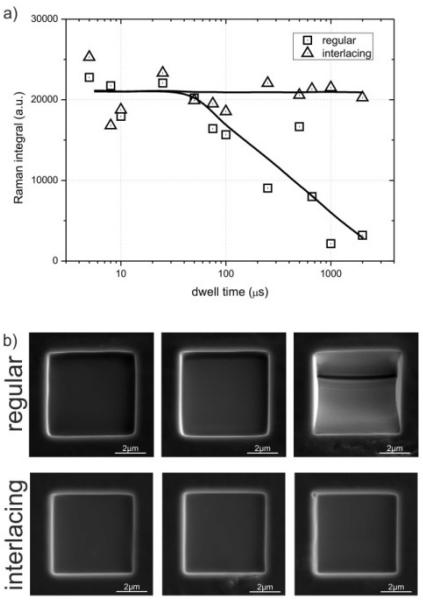

Figure S 2:a) Raman integral for EVA for regular (squares) and interlaced (triangles) patterning depending on the dwell time (in logarithmic abscise); b) SEM images of the morphology achieved on EVA for low (left), medium (middle) and high (right) dwell times, when a regular patterning strategy is used.

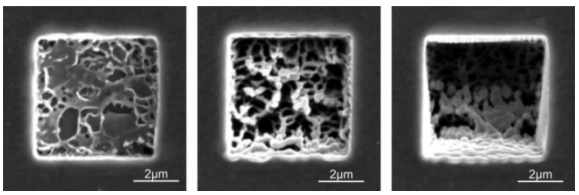

Figure S 3: SEM images of 5 x 5 µm squares on PEG for low (left), medium (middle) and high (right) dwell times; the morphological development is clearly that of a polymer that rather undergoes chain scission.

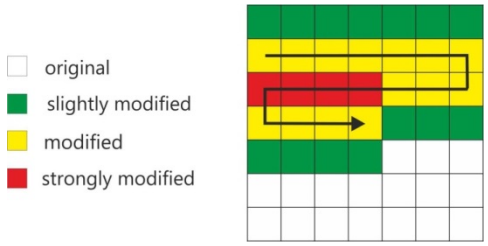

Figure S 4: top view of material distribution after patterning with serpentine strategies (arrow). As can be seen, the material distribution is strongly asymmetric with respect to the actual ion beam position and scan direction. Modification code is shown at the left.

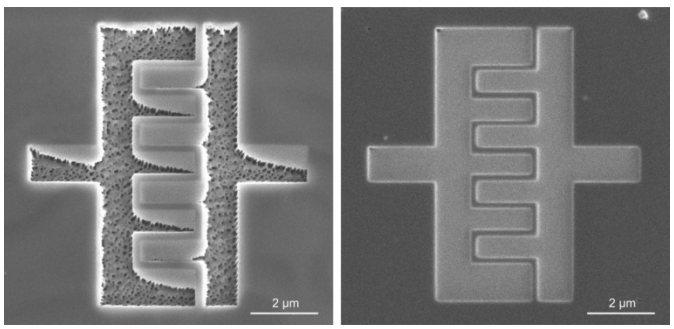

Figure S 5: regular serpentine (left) and smart interlacing (right) structuring results on PMMA performed with a low ion beam current of 100 pA at 30 kV, 35 nm PoP / PoP_F, 60 nm PoP_{IL}, 2 ms DT via single loop with identical process time (scale bar is XX µm).

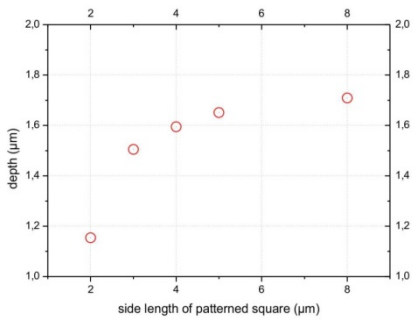

Figure S 6: depth versus side length of the used quadratic patterning footprints. As can be seen for sizes below 4 µm the milling rate decreases due to re-deposition effects.